Deep donor state of the copper acceptor as a source of green luminescence in ZnO

J. L. Lyons, A. Alkauskas, A. Janotti, and C. G. Van de Walle

Citation: Appl. Phys. Lett. **111**, 042101 (2017); doi: 10.1063/1.4995404
View online: http://dx.doi.org/10.1063/1.4995404
View Table of Contents: http://aip.scitation.org/toc/apl/111/4
Published by the American Institute of Physics

Deep donor state of the copper acceptor as a source of green luminescence in ZnO

J. L. Lyons,[1] A. Alkauskas,[2] A. Janotti,[3] and C. G. Van de Walle[4]
[1]Center for Computational Materials Science, Naval Research Laboratory, Washington, DC 20375, USA
[2]Center for Physical Sciences and Technology, Vilnius LT-10257, Lithuania
[3]Department of Materials Science and Engineering, University of Delaware, Newark, Delaware 19716, USA
[4]Materials Department, University of California, Santa Barbara, California 93106-5050, USA

(Received 1 May 2017; accepted 10 July 2017; published online 24 July 2017)

Copper impurities have long been linked with green luminescence (GL) in ZnO. Copper is known to introduce an acceptor level close to the conduction band of ZnO, and the GL has conventionally been attributed to transitions involving an excited state which localizes holes on neighboring oxygen atoms. To date, a theoretical description of the optical properties of such deep centers has been difficult to achieve due to the limitations of functionals in the density functional theory. Here, we employ a screened hybrid density functional to calculate the properties of Cu in ZnO. In agreement with the experiment, we find that Cu_{Zn} features an acceptor level near the conduction band of ZnO. However, we find that Cu_{Zn} also gives rise to a deep *donor* level 0.46 eV above the valence band of ZnO; the calculated optical transitions involving this state agree well with the GL observed in ZnO:Cu. [http://dx.doi.org/10.1063/1.4995404]

The properties of copper impurities in ZnO have been studied extensively since the 1960s.[1–10] These investigations have partly been driven by the general interest in acceptors and potential *p*-type dopants in ZnO. Cu has also been intentionally doped into ZnO to give nonlinear current-voltage characteristics[11,12] useful for varistors to create highly resistive films for piezoelectric applications[13] and also to create phosphorescent thin films.[14] Cu-doped ZnO was also recently employed to create low-power H_2 sensors.[15]

Doping studies,[4,5] electron paramagnetic resonance (EPR) measurements,[1] and admittance spectroscopy[16] indicate that copper on a Zn site (Cu_{Zn}) has an acceptor level (i.e., a transition between a neutral and a – charge state) ∼0.2 eV below the conduction-band minimum (CBM) in ZnO. Thus, Cu_{Zn} has an ionization energy of 3.2 eV when referenced to the valence-band maximum (VBM). Acceptors are usually expected to give rise to levels near the VBM; the large ionization energy makes Cu_{Zn} an exceedingly deep acceptor, ruling out its use for *p*-type doping.

Cu_{Zn} has also long been known to be a source of the green luminescence (GL) observed around 2.4–2.5 eV.[2] Previous EPR studies[1] showed that Cu incorporates on the Zn site, where it acts as a deep acceptor with states composed of 3*d* levels [see Fig. 1(a)]. The attribution of the GL to Cu_{Zn} was later made by Dingle,[2] who described the luminescence process as a transfer of a hole bound to nearest neighbor oxygen atoms in the excited state to the localized levels of Cu_{Zn} (i.e., the ground state of Cu_{Zn}). Dingle observed a zero-phonon line (ZPL) at 2.86 eV and a peak photoluminescence (PL) energy of 2.48 eV along with distinct phonon replicas and estimated that the excited state of Cu_{Zn} should occur about 450 meV above the VBM of ZnO.[2] Finally, since the ground state of the transition (Cu^0_{Zn}) was present in the unexcited sample, the acceptor ionization energy was surmised to be very large. Subsequent experimental studies of ZnO:Cu concurred with the original description by Dingle,[3–5,8,10,17] and reported similar GL with distinct phonon replicas (i.e., a "structured" PL band). These replicas distinguish the Cu-related GL band from the relatively featureless GL signals also observed in ZnO which likely originate from a different source.[18]

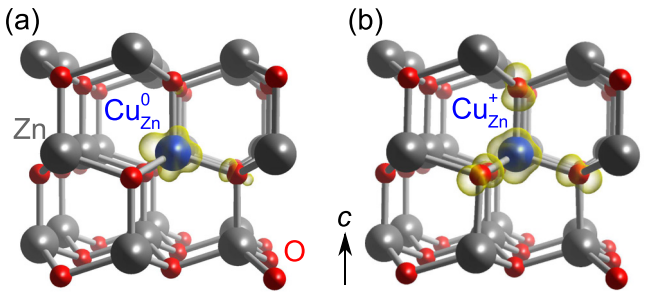

FIG. 1. Local lattice configurations of copper in the (a) Cu^0_{Zn} and (b) Cu^+_{Zn} charge states in ZnO. In both cases, the yellow isosurface represents the spin density and is set to 5% of the maximum.

Attempts to corroborate this picture with first-principles calculations have been stymied by the inability of the theoretical approaches to accurately describe deep levels, particularly those that involve highly localized electronic states. The density functional theory (DFT) based on the local density approximation (LDA) or the generalized gradient approximation (GGA) accurately predicts the structural properties of materials, but both LDA and GGA fail to correctly describe the electronic band structure of wide-band-gap semiconductors and charge localization onto defects.[19] In the case of ZnO:Cu_{Zn}, LDA calculations found a (0/–) acceptor level at 0.7 eV above the VBM,[6] much lower than the experimentally observed value.

Great progress has recently been made through the application of hybrid functionals, which have been demonstrated to accurately describe band structures and correctly predict charge localization.[19–21] Indeed, a study of ZnO:Cu employing the B3LYP hybrid functional[9] predicted an acceptor level at 2.48 eV, much deeper than the LDA results.[6] A study employing an LDA + *U*-inspired method

(which partially corrects the band gap) also predicted much deeper Cu_{Zn} levels,[7] although the ultimate value depended on the details of the correction scheme. Another DFT + U study (based on GGA + U), in conjunction with PL experiments, identified a Cu^{3+} ion as a final state of the GL[22] but did not report transition levels.

In this work, we employ a hybrid functional to study the Cu acceptor in ZnO. Our calculations are based on the generalized Kohn-Sham scheme[23] with the hybrid functional of Heyd, Scuseria, and Ernzerhof (HSE),[24,25] as implemented in the Vienna *Ab-Initio* Simulation Package (VASP),[26] in which a fraction of exact exchange is mixed with the short-range GGA exchange potential of Perdew, Burke, and Ernzerhof (PBE).[27] The mixing parameter for the Hartree-Fock potential is set to 0.36, and the screening length is set to the standard 0.2 $Å^{-1}$, resulting in a band gap of 3.35 eV, which is in good agreement with the experimental value.[28] Although a different combination of parameters could in principle correctly describe the bulk band structure, such an exploration of the full parameter space is beyond the scope of this work. HSE has also been demonstrated to produce structural parameters that are also close to the experiment.[29] The interactions between the valence electrons and the ionic cores are described using the projector-augmented wave (PAW) method.[30,31] Cu_{Zn} calculations are performed using a 96-atom supercell, a plane-wave basis set with a cutoff of 400 eV, and a $2 \times 2 \times 2$ special k-point set for integrations over the Brillouin zone. Spin polarization is explicitly included. Symmetry-breaking distortions are introduced, and atomic relaxations are consistently performed using the HSE functional. Structures are considered converged when Hellman-Feynman forces are lower than 0.02 eV/Å.

We calculate formation energies of the impurity in various charges using the well-established formalism described in Ref. 19. The formation energy of copper on the zinc site (Cu_{Zn}) in charge state q is given by

$$E^f(Cu^q_{Zn}) = E_{tot}(Cu^q_{Zn}) - E_{tot}(ZnO) + \mu_{Zn} - \mu_{Cu} + q(E_F + \varepsilon_v) + \Delta^q, \quad (1)$$

in which $E_{tot}(Cu^q_{Zn})$ is the total energy of a supercell containing a single Cu^q_{Zn} in charge state q and E_{tot} (ZnO) is the total energy of a pristine supercell. Electrons that are added or removed from the supercell are exchanged with the Fermi level (E_F) of the semiconductor host which is referenced to the VBM (ε_v), and Δ^q corresponds to a correction for the finite size of charged supercells.[32,33] μ_{Zn} and μ_{Cu} are referenced to the energy of an atom in their respective bulk metals. Both are treated as variables that must satisfy the stability conditions

$$\mu_{Zn} + \mu_O = \Delta H_f(ZnO), \quad (2)$$

and

$$\mu_{Cu} + \mu_O = \Delta H_f(CuO), \quad (3)$$

for which ΔH_f(ZnO) = –3.66 eV and ΔH_f(CuO) = –1.63 eV.[34] In Fig. 2, we plot the formation energy of Cu_{Zn} under two conditions, Zn-rich (at which μ_{Zn} = 0 eV) and O-rich (at which μ_O = 0 eV). We find that Cu_{Zn} in ZnO is most stable under O-rich conditions.

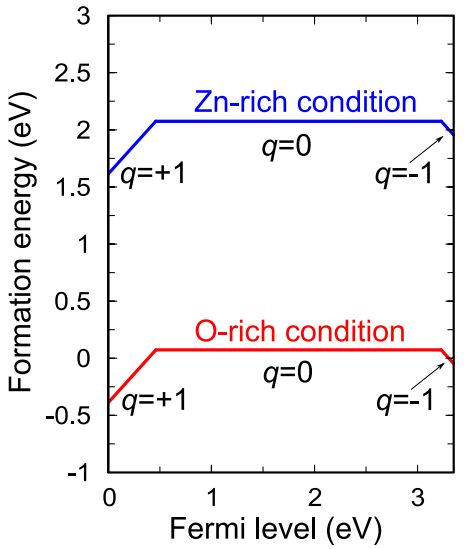

FIG. 2. Formation energy of Cu_{Zn} as a function of the Fermi level in ZnO under Zn-rich (blue lines) and O-rich (red lines) conditions.

The thermodynamic transition level between charge states q and q' of the impurity is then given by the Fermi-level position at which the formation energy of the impurity in charge state q is equal to that in charge state q'. In the case of Cu_{Zn}, the (0/–) transition level (which corresponds to the ionization energy) is given by[19]

$$(0/-) = E^f(Cu^-_{Zn}; E_F = 0) - E^f(Cu^0_{Zn}). \quad (4)$$

where $E^f(Cu^-_{Zn}; E_F = 0)$ is the formation energy of Cu^-_{Zn} when the Fermi level is at the VBM and $E^f(Cu^0_{Zn})$ is the formation energy of Cu^0_{Zn} (which does not vary with the Fermi level).

This transition level represents a thermal ionization energy and should not be confused with optical transition levels, whose energies can differ considerably from ionization energies. Peak transition energies and peak widths can be estimated from configuration coordinate diagrams (as explained in Ref. 19). We also calculate full luminescence lineshapes including vibronic coupling using the procedure outlined in Ref. 35.

Cu acceptors incorporating on the Zn site have a deficit of one electron relative to Zn. In the negative charge state (i.e., with all levels filled), Cu_{Zn} produces levels deep in the band gap which are composed of Cu 3d states. When an electron is removed from the system to create the neutral charge state, the resulting hole is localized mainly on the Cu impurity (from a projection onto the PAW spheres, we estimate that the unpaired electron has a 95% Cu 3d character). The nature of this state is also illustrated by the spin density in Fig. 1(a); it is localized mostly onto Cu_{Zn}, with the 3d character, with a small fraction of the spin density occurring on a neighboring O atom. We calculate the (0/–) transition level to be 3.27 eV above the VBM.

Removal of a second electron leads to the Cu^+_{Zn} charge state, which has a total magnetic moment of 2 (i.e., two unpaired electrons). As can be seen in Fig. 1(b), this state

has a strong O 2*p* character in addition to Cu 3*d* (we estimate the character to be 60% Cu 3*d* and 40% O 2*p*). The involvement of O-2*p* states is consistent with the positive charge state being stable only for Fermi levels near the VBM as shown in Fig. 2; we calculate that the (+/0) transition level occurs at 0.46 eV above the VBM. A similar near-VBM deep-donor transition level was previously reported for Cu_{Zn} in ZnO.[7]

Various charge states of Cu_{Zn} exhibit very different local lattice relaxations. For Cu_{Zn}^{-}, all nearest neighbor O atoms relax outwards, one by 6% and the other three by 5% of the bulk bond length. In contrast, for Cu_{Zn}^{0}, one neighboring O atom relaxes inwards by 2% of the bulk bond length, another moves outward by 5%, and the other two remain almost unchanged. For Cu_{Zn}^{+}, all neighboring O atoms move inwards, three by 6% of the bulk bond length, and one by 3%. In all cases, the Cu atom remains in the vicinity of the Zn substitutional site.

We now examine optical transitions related to Cu_{Zn}. The configuration coordinate diagrams shown in Fig. 3 address both recombinations of a hole with the – charge state and of an electron with the + charge state. The large difference in atomic configurations between the three Cu_{Zn} charge states gives rise to sizeable relaxation energies, causing the peak energies of the optical transitions to be very different from the thermodynamic transition levels (which determine the ZPL) and leading to broad PL bands. For the processes related to the (0/–) level [Fig. 3(a)], the absorption peak (to lift an electron out of the VBM and make the impurity negatively charged) occurs at 3.85 eV, with a relaxation energy of 0.58 eV. For the emission process (involving the electron on Cu_{Zn}^{-} recombining with a hole at the VBM), we find a peak at 2.58 eV, with a relaxation energy of 0.69 eV.

Although this luminescence peak is close to the experimentally observed values (2.48 eV in Ref. 2, 2.43 eV in Ref. 17, and 2.39 eV in Ref. 10), its associated ZPL (3.27 eV) is nearly 0.4 eV larger than the experimental ZPL at 2.86 eV.[2] We also note that the 3.27 eV ZPL of the (0/–) transition level is not consistent with the 2.9 eV PL excitation onset reported in Ref. 10.

In Fig. 3(b), we consider the recombination of an electron from the conduction band with the positive charge state of Cu_{Zn}. For this transition, we predict an absorption peak of 3.37 eV, an emission peak of 2.31 eV, and relaxation energies of 0.48 and 0.58 eV. The ZPL, at 2.89 eV, is in excellent agreement with the observed ZPL at 2.86 eV[2] and with the onset of the PLE spectrum in Ref. 10. The emission peak differs from the GL peaks observed in the experiment[2,10,17] by ∼0.1 eV, but we note that the value extracted from a configuration coordinate diagram is only an approximation. The calculation of the full luminescence lineshape, using the formalism described in Ref. 35, offers a more accurate assessment.

The calculated luminescence lineshapes for the optical transitions described in Fig. 3 are shown in Fig. 4. We compare these with the experimental spectra observed in Ref. 36 by normalizing the luminescence intensities. The $(- \rightarrow 0)$ optical transition gives rise to a broad PL signal peaking at 2.54 eV, while the $(+ \rightarrow 0)$ transition gives rise to a narrower PL signal peaking at 2.39 eV. Since our calculations are based on the effective one-dimensional configuration-coordinate picture,[35] they yield the overall shape of the luminescence band but not its detailed fine structure.

The calculated vibrational parameters[37] for the luminescence lineshapes are listed in Table I. The calculated vibrational frequencies for the $(- \rightarrow 0)$ and $(+ \rightarrow 0)$ transitions are similar and also close to frequencies of the structured GL observed in ZnO (64 meV in Ref. 36). The smaller Huang-Rhys factor of the $(+ \rightarrow 0)$ transition is consistent with our expectation that this level gives rise to the structured GL observed in ZnO:Cu (since a smaller Huang-Rhys factor leads to more structured lineshapes[38]). We note that the Huang-Rhys factors of Cu_{Zn} are smaller than those we have previously calculated for other acceptors in ZnO (which have $S > 15$).[35,39]

Finally, we note that our proposed mechanism for the Cu-related GL is distinct from that of Dingle.[2] The mechanism that we propose is based on the (+/0) transition level of Cu_{Zn} [Fig. 1(b)], which had not been previously considered as a source for the GL. The initial state of this transition features hole localization onto O nearest neighbors, similar to what was proposed in Ref. 2. However, the transition we propose here is based on the Cu_{Zn}^{+} charge state, while Dingle focused on an excited state of Cu_{Zn}^{0}. Our attempts to stabilize such an excited state for Cu_{Zn^0} were not successful. We also note that Cu_{Zn}^{+} was recently proposed to be the final state of the GL in ZnO[22] in a combined experimental and theoretical study. Reference 22 did not provide information about transition levels but focused on the doublet structure, i.e., a ZPL

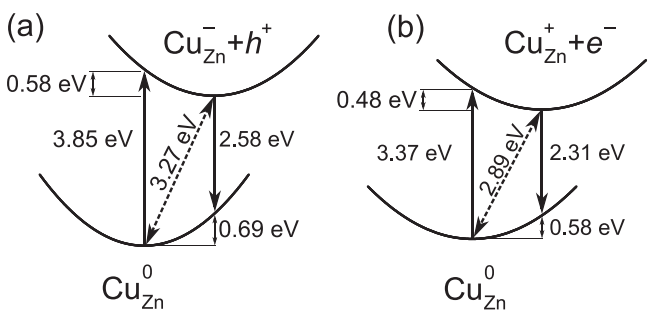

FIG. 3. Calculated configuration coordinate diagrams for Cu_{Zn} in ZnO for (a) the recombination of a hole into the (0/–) level and (b) the recombination of an electron into the (+/0) level.

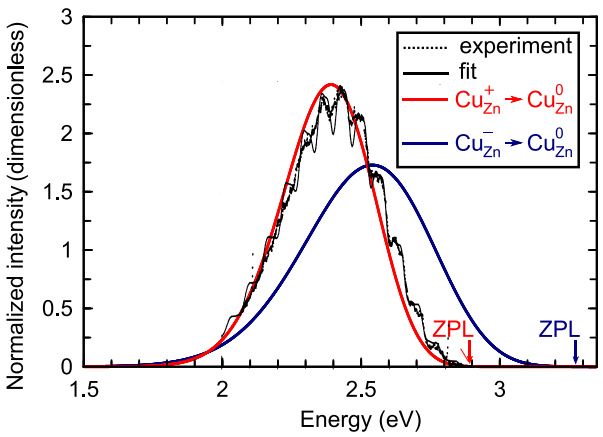

FIG. 4. Calculated luminescence lineshapes for the $(+ \rightarrow 0)$ transition (in red) and the $(- \rightarrow 0)$ transition in blue for Cu_{Zn}, compared with the spectra observed (dotted black line) and fitted (solid black line) in Ref. 36.

TABLE I. Calculated Huang-Rhys factors (S_g) and effective vibrational frequencies in the ground state ($\hbar\Omega_g$) and in the excited state ($\hbar\Omega_e$) for the two Cu_{Zn}-related optical transitions.

Parameter	$(- \rightarrow 0)$	$(+ \rightarrow 0)$
S_g	13.1	11.1
$\hbar\Omega_g$ (meV)	57	52
$\hbar\Omega_e$ (meV)	46	53

splitting of 0.11 meV (which was attributed to isotopic effects by Dingle). Investigating such a fine structure is beyond the scope of our present work.

In conclusion, we have determined the properties of the copper acceptor in ZnO using the HSE hybrid functional. We find that Cu_{Zn} has an acceptor level near the CBM of ZnO, in agreement with experiment. However, we find that Cu_{Zn} also gives rise to a deep donor level 0.46 eV above the VBM. Electron recombination into this level is found to give rise to 2.31 eV green luminescence in ZnO within our 1D configuration-coordinate diagram. Our calculated full luminescence lineshape is in excellent agreement with the experiment for this transition, with a peak luminescence of 2.39 eV and a ZPL of 2.89 eV.

The work at UCSB was supported by the U. S. Department of Energy (DOE), Office of Science, Basic Energy Sciences (BES) under Award No. DE-SC0010689. A.A. acknowledges support by Marie Sklodowska-Curie Action of the European Union (project NITRIDE-SRH, Grant No. 657054). Computational resources were provided by the Center for Scientific Computing at the California Nanosystems Institute and Materials Research Laboratory (an NSF Materials Research Science and Engineering Center, DMR-1121053) (NSF CNS-0960316) and by the National Energy Research Scientific Computing Center, a DOE Office of Science User Facility under Contract No. DE-AC02–05CH11231. J.L.L. acknowledges support from the Office of Naval Research through the Naval Research Laboratory's Basic Research Program, and computational support from the DoD Major Shared Resource Center at AFRL.

[1]R. E. Dietz, H. Kamimura, M. D. Sturge, and A. Yariv, Phys. Rev. **132**, 1559 (1963).
[2]R. Dingle, Phys. Rev. Lett. **23**, 579 (1969).
[3]G. Baur, E. V. Freydorf, and W. H. Koscherl, Phys. Status Solidi A **21**, 247 (1974).
[4]G. Müller, Phys. Status Solidi B **76**, 525 (1976).
[5]D. J. Robbins, P. J. Dean, P. E. Simmons, and H. Tews, in *Deep Centers in Semiconductors*, 2nd ed., edited by S. Pantelides (Gordon and Breach, New York, 1986), pp. 843–898.
[6]Y. Yan, M. M. Al-Jassim, and S.-H. Wei, Appl. Phys. Lett. **89**, 181912 (2006).
[7]S. Lany and A. Zunger, Phys. Rev. B **80**, 085202 (2009).
[8]M. A. Reshchikov, V. Avrutin, N. Izyumskaya, R. Shimada, H. Morkoç, and S. W. Novak, J. Vac. Sci. Technol., B **27**, 1749 (2009).
[9]F. Gallino and C. Di Valentin, J. Chem. Phys. **134**, 144506 (2011).
[10]M. D. McCluskey, C. D. Corolewski, J. Lv, M. C. Tarun, S. T. Teklemichael, E. D. Walter, M. G. Norton, K. W. Harrison, and S. Ha, J. Appl. Phys. **117**, 112802 (2015).
[11]T. R. N. Kutty and N. Raghu, Appl. Phys. Lett. **54**, 1796 (1989).
[12]B.-S. Chiou and M.-C. Chung, J. Am. Ceram. Soc. **75**, 3363 (1992).
[13]M. Labeau, P. Rey, J. L. Deschanvres, J. C. Joubert, and G. Delabouglise, Thin Solid Films **213**, 94 (1992).
[14]T. G. Kryshtab, V. S. Khomchenko, V. P. Papusha, M. O. Mazin, and Y. A. Tzurkunov, Thin Solid Films **403–404**, 76 (2002).
[15]L. Chow, O. Lupan, G. Chai, H. Khallaf, L. K. Ono, B. R. Cuenya, I. M. Tiginyanu, V. V. Ursaki, V. Sontea, and A. Schulte, Sens. Actuators, A **189**, 399 (2013).
[16]Y. Kanai, Jpn. J. Appl. Phys., Part 1 **30**, 703 (1991).
[17]N. Y. Garces, L. Wang, L. Bai, N. C. Giles, L. E. Halliburton, and G. Cantwell, Appl. Phys. Lett. **81**, 622 (2002).
[18]K. Vanheusden, W. L. Warren, C. H. Seager, D. R. Tallant, J. A. Voigt, and B. E. Gnade, J. Appl. Phys. **79**, 7983 (1996).
[19]C. Freysoldt, B. Grabowski, T. Hickel, J. Neugebauer, G. Kresse, A. Janotti, and C. G. Van de Walle, Rev. Mod. Phys. **86**, 253 (2014).
[20]A. Carvalho, A. Alkauskas, A. Pasquarello, A. K. Tagantsev, and N. Setter, Phys. Rev. B **80**, 195205 (2009).
[21]J. L. Lyons, A. Janotti, and C. G. Van de Walle, J. Appl. Phys. **115**, 012014 (2014).
[22]H. Ye, Z. Su, F. Tang, M. Wang, G. Chen, J. Wang, and S. Xu, Sci. Rep. **7**, 41460 (2017).
[23]W. Kohn and L. Sham, Phys. Rev. **140**, A1133 (1965).
[24]J. Heyd, G. E. Scuseria, and M. Ernzerhof, J. Chem. Phys. **118**, 8207 (2003).
[25]J. Heyd, G. E. Scuseria, and M. Ernzerhof, J. Chem. Phys. **124**, 219906 (2006).
[26]G. Kresse and J. Furthmüller, Phys. Rev. B **54**, 11169 (1996).
[27]J. P. Perdew, K. Burke, and M. Ernzerhof, Phys. Rev. Lett. **77**, 3865 (1996).
[28]*Semiconductors - Basic Data*, 2nd revised ed., edited by O. Madelung (Springer, Berlin, 1996).
[29]J. L. Lyons, A. Janotti, and C. G. Van de Walle, Appl. Phys. Lett. **95**, 252105 (2009).
[30]P. E. Blöchl, Phys. Rev. B **50**, 17953 (1994).
[31]G. Kresse and J. Joubert, Phys. Rev. B **59**, 1758 (1999).
[32]C. Freysoldt, J. Neugebauer, and C. G. Van de Walle, Phys. Rev. Lett. **102**, 016402 (2009).
[33]C. Freysoldt, J. Neugebauer, and C. G. Van de Walle, Phys. Status Solidi B **248**, 1067 (2011).
[34]*CRC Handbook of Chemistry and Physics*, 84th ed., edited by D. R. Lide (CRC Press, Boca Raton, FL, 2003).
[35]A. Alkauskas, J. L. Lyons, D. Steiauf, and C. G. Van de Walle, Phys. Rev. Lett. **109**, 267401 (2012).
[36]D. C. Reynolds, D. C. Look, and B. Jogai, J. Appl. Phys. **89**, 6189 (2001).
[37]A. M. Stoneham, *Theory of Defects in Solids: Electronic Structure of Defects in Insulators and Semiconductors* (Oxford University Press, Oxford, 1975).
[38]A. Alkauskas, M. D. McCluskey, and C. G. Van de Walle, J. Appl. Phys. **119**, 181101 (2016).
[39]A. Alkauskas, Q. Yan, and C. G. Van de Walle, Phys. Rev. B **90**, 075202 (2014).